AMERICAN SOCIETY FOR MICROBIOLOGY | mBio®

RESEARCH ARTICLE

Listeria InlB Expedites Vacuole Escape and Intracellular Proliferation by Promoting Rab7 Recruitment via Vps34

Robert J. Cain,[a] Mariela Scortti,[a] Héctor J. Monzó,[a]* José A. Vázquez-Boland[a]

[a]Microbial Pathogenesis Laboratory, Infection Medicine, Edinburgh Medical School (Biomedical Sciences), University of Edinburgh, Edinburgh, Scotland, United Kingdom

ABSTRACT Rapid phagosomal escape mediated by listeriolysin O (LLO) is a prerequisite for *Listeria monocytogenes* intracellular replication and pathogenesis. Escape takes place within minutes after internalization from vacuoles that are negative to the early endosomal Rab5 GTPase and positive to the late endosomal Rab7. Using mutant analysis, we found that the listerial invasin InlB was required for optimal intracellular proliferation of *L. monocytogenes*. Starting from this observation, we determined in HeLa cells that InlB promotes early phagosomal escape and efficient Rab7 acquisition by the *Listeria*-containing vacuole (LCV). Recruitment of the class III phosphoinositide 3-kinase (PI3K) Vps34 to the LCV and accumulation of its lipid product, phosphatidylinositol 3-phosphate (PI3P), two key endosomal maturation mediators, were also dependent on InlB. Small interfering RNA (siRNA) knockdown experiments showed that Vps34 was required for Rab7 recruitment and early (LLO-mediated) escape and supported InlB-dependent intracellular proliferation. Together, our data indicate that InlB accelerates LCV conversion into an escape-favorable Rab7 late phagosome via subversion of class III PI3K/Vps34 signaling. Our findings uncover a new function for the InlB invasin in *Listeria* pathogenesis as an intracellular proliferation-promoting virulence factor.

IMPORTANCE Avoidance of lysosomal killing by manipulation of the endosomal compartment is a virulence mechanism assumed to be largely restricted to intravacuolar intracellular pathogens. Our findings are important because they show that cytosolic pathogens like *L. monocytogenes*, which rapidly escape the phagosome after internalization, can also extensively subvert endocytic trafficking as part of their survival strategy. They also clarify that, instead of delaying phagosome maturation (to allow time for LLO-dependent disruption, as currently thought), via InlB *L. monocytogenes* appears to facilitate the rapid conversion of the phagocytic vacuole into an escape-conducive late phagosome. Our data highlight the multifunctionality of bacterial virulence factors. At the cell surface, the InlB invasin induces receptor-mediated phagocytosis via class I PI3K activation, whereas after internalization it exploits class III PI3K (Vsp34) to promote intracellular survival. Systematically elucidating the mechanisms by which *Listeria* interferes with PI3K signaling all along the endocytic pathway may lead to novel anti-infective therapies.

KEYWORDS *Listeria monocytogenes*, *Listeria* virulence, internalins, InlB, intracellular parasitism, intracellular survival, intracellular proliferation, endocytic trafficking, phagosome maturation, *Listeria*-containing vacuole, vacuole escape, subversion of phosphoinositide metabolism, phosphoinositide 3-kinase, class III PI3K, Vps34, phosphatidylinositol 3-phosphate, Rab5, Rab7

The Gram-positive pathogen *Listeria monocytogenes* is the causative agent of listeriosis, an invasive foodborne infection with severe clinical manifestations, including meningoencephalitis, septicemia, stillbirth, and neonatal sepsis (1). *Listeria* virulence depends on the ability of these bacteria to proliferate within macrophages and a variety of nonphagocytic cells. In contrast to other major intracellular pathogens, such as

Editor Scott J. Hultgren, Washington University School of Medicine

Address correspondence to José A. Vázquez-Boland, v.boland@ed.ac.uk.

*Present address: Héctor J. Monzó, Translational Cancer Medicine Research Program, Biomedicum 1, Faculty of Medicine, University of Helsinki, Helsinki, Finland.

The authors declare no conflict of interest.

This article is a direct contribution from Jose A. Vazquez-Boland, a Fellow of the American Academy of Microbiology, who arranged for and secured reviews by Anna Oevermann, University of Bern, Switzerland, and Si Ming Man, The Australian National University.

Received 21 November 2022
Accepted 8 December 2022

Mycobacterium tuberculosis or *Salmonella*, *Listeria* replicates in the cytosol and not in a membrane-bound vacuole (2, 3).

Within 30 min of cell entry, *Listeria* bacteria escape from acidified vesicles (4) bearing characteristics of late endosomes prior to fusion with lysosomes (Rab5 negative, Rab7 positive, and lysosomal-associated membrane protein 1 [LAMP1] negative) (5). This process is mediated by the listerial *hly* gene product, the pore-forming toxin listeriolysin O (LLO), upon its activation at acidic pH (5.5 to 6.0), aided by phospholipases PlcA and PlcB (6). Rapid multiplication ensues, fueled by hexose phosphates, which *Listeria* take up from the cytosol via the Hpt permease (7). After replication, the listerial actin-polymerizing protein ActA induces actin-based motility and cell-to-cell spread (8), allowing cytosolic *Listeria* to escape from autophagy (9) and to disseminate throughout host tissues while remaining protected from extracellular defenses (10). InlC, a member of the listerial internalin family (11), cooperates with ActA in cell-to-cell spread (12) while dampening innate immunity by inhibiting NF-κB responses (13).

Active invasion of epithelial and other normally nonphagocytic cells is critical for host barrier translocation and parenchymal tissue colonization by *Listeria*. Entry into these cells is mediated by the products of the *L. monocytogenes inlAB* operon, the surface-associated internalins InlA and InlB (14). InlA and InlB interact with specific host cell ligands, the junctional adhesion protein E-cadherin (15, 16) and the hepatocyte growth factor (HGF) receptor Met (17, 18), respectively, triggering phagocytosis. While both internalins synergize and are required for full *L. monocytogenes* invasiveness, InlA is thought to be specifically important for internalization into certain human epithelial cell subpopulations, whereas InlB promotes entry into a broader range of cell types (19, 20). The entry process begins with the ubiquitination of the InlA and InlB receptors, followed by recruitment of the actin cytoskeleton at clathrin-coated bacterial adhesion sites, with myosin VI providing the force for internalization (21–23). Subsequently, InlB reinforces the cortical actin polymerization cascade via activation of class I phosphoinositide 3-kinase (PI3K) downstream of Met (24), with accumulation of phosphatidylinositol 3,4,5-triphosphate (PI[3,4,5]P_3) in the cell membrane, local recruitment of small Rho family GTPases and actin-binding proteins, and phagosome formation (reviewed in reference 25).

The *Listeria* intracellular survival-promoting determinants (LLO, PlcA, PlcB, Hpt, ActA, InlC) are coordinately regulated by the transcriptional activator PrfA (26). Consistent with their primary intracellular function, PrfA-regulated genes are weakly expressed extracellularly and selectively activated within host cells (27). Interestingly, although having an established role in cell entry, the *inlAB* locus is also controlled by PrfA (28) and its expression is activated during intracellular infection (29, 30; our unpublished results), suggesting a potential function following internalization. We investigated the possible involvement of the *inlAB* products in *L. monocytogenes* intracellular proliferation in human epithelial cells. Here, we report that the invasin InlB promotes early phagosomal escape, and hence bacterial intracellular proliferation, by accelerating the formation of a late-endosomal Rab7-positive compartment via subversion of class III PI3K signaling.

RESULTS

InlB is required for efficient intracellular proliferation. Isogenic *L. monocytogenes* in-frame *inlA* and *inlB* deletion mutants were tested in human epithelial HeLa cells using gentamicin protection assays. Since the intracellular population at a given time point depends directly on the initial number of internalized bacteria, the multiplicity of infection (MOI) was adjusted such that each strain had comparable intracellular numbers at $t = 0$ (average of $\sim 5 \times 10^4$ colony forming units [CFU]/well). In addition, the intracellular proliferation data were normalized to the bacterial counts at $t = 0$ using an intracellular growth coefficient (IGC) (27) (see Materials and Methods).

As shown in Fig. 1A, while the Δ*inlA* mutant behaved as the wild type (WT), a distinct intracellular growth defect was observed for the Δ*inlB* mutant. This was reproduced in other cell lines (human intestinal Caco-2 cells, murine J774 macrophages) (see Fig. S1 in the supplemental material) and corroborated early observations in mouse hepatocytes (31).

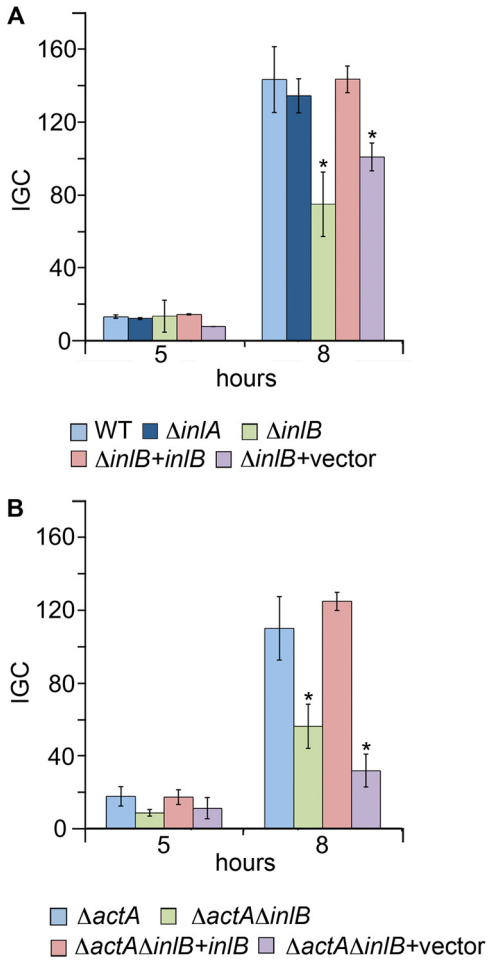

FIG 1 InlB is required for efficient intracellular proliferation of *L. monocytogenes*. Intracellular CFU of WT, Δ*inlA*, and Δ*inlB* in HeLa cells were normalized at each time point to the internalized bacterial CFU at $t = 0$ using an intracellular growth coefficient (IGC) (see Materials and Methods). *, significant difference from WT ($P < 0.05$). (A) Data for WT, Δ*inlA*, Δ*inlB*, and *inlB*- or mock-complemented Δ*inlB* bacteria. Corresponding mean CFU/well ($\times 10^4$) at $t = 0$ for the respective strains: 4.9 ± 1.8, 1.4 ± 0.13, 4.6 ± 1.7, 6.1 ± 4.8, and 3.9 ± 2.4. (B) Experiments in the cell-to-cell spread-null (Δ*actA*) background. Corresponding mean CFU/well ($\times 10^4$) at $t = 0$: Δ*actA*, 4.4 ± 1.7; Δ*actA* Δ*inlB*, 3.8 ± 2.4; Δ*actA* Δ*inlB*+*inlB*, 4.3 ± 2.6; Δ*actA* Δ*inlB*+vector, 3.7 ± 2.6.

The effect was not attributable to impaired bacterial fitness, since the Δ*inlB* mutant showed no growth defect in broth (Fig. S1B). Complementation of Δ*inlB* with the *inlB* gene on a plasmid, but not empty vector, rescued InlB production (Fig. S1C), normal cell entry (Fig. S1D), and WT intracellular proliferation (Fig. 1A), linking the observed phenotype to InlB.

L. monocytogenes proliferation in a cell monolayer is dependent on both successful escape to the cytosol and actin-based spreading to adjacent cells. The contribution of cell-to-cell spread to the Δ*inlB* proliferation defect can be tested using a strain lacking ActA (8). While, as expected, overall proliferation was generally reduced in the absence of ActA due to the spread deficiency, intracellular growth was significantly diminished in a Δ*actA* Δ*inlB* double mutant compared to the Δ*actA* single mutant. Again, complementation with *inlB*, but not empty vector, reverted the proliferation defect (Fig. 1B). Together, these data indicated that the absence of InlB impairs *L. monocytogenes* intracellular proliferation due to effects upstream of cell-to-cell spread.

InlB promotes early vacuole escape. The Δ*inlB* phenotype could be due either to a reduced ability to replicate within the cytoplasm or to an earlier defect in vacuole escape. To test this, the proportion of vacuole-associated and cytosolic bacteria was monitored over a 90-min infection time course in HeLa cells using two separate

microscopy-based assays. Vacuole-associated bacteria were identified by colocalization with FM 1-43FX, a fluorescent membrane probe that constitutively labels endosomes and phagosomes (32, 33). The vacuole marker was associated as early as 10 min after infection with WT *L. monocytogenes*, with a peak at 20 to 30 min before rapidly dropping to ~20% of the bacterial population by 90 min (Fig. 2A and B). Although entering in fewer numbers (Fig. S2B), the Δ*inlB* bacteria that successfully invaded the monolayer showed similar FM 1-43FX colocalization dynamics during the first 30 to 45 min of infection. Subsequently, however, the Δ*inlB* mutant remained membrane associated in high numbers, the percentage only dropping by 20% over the rest of the time course (Fig. 2A and Fig. S2A). To quantify the phenotype while controlling for variations in cell entry rate, vacuolar persistence (VP) was calculated based on the length of time between 50% initial bacterial association and 50% dissociation with the membrane probe relative to peak values. The VP values were 34.2 ± 8.0 and 69.6 ± 5.0 min for the WT and Δ*inlB* mutant, respectively (Fig. 2A, right), suggesting the latter had a vacuole escape defect. In parallel, cytosolic bacteria were identified both through ActA-mediated F-actin accumulation (8) and decoration with a transfected fluorescent probe that binds to *Listeria* after escape to the cytosol (CBD, a listeriophage endolysin cell wall-binding domain fused to yellow fluorescent protein [YFP]) (5). Consistent with the vacuole association data, significant decoration with the CBD probe was observed later for the Δ*inlB* mutant than the WT. The dynamics of actin accumulation around bacteria mirrored the CBD probe data (Fig. 2C and D). With both approaches, the mutant phenotype reverted to WT in the *inlB*-complemented Δ*inlB* mutant (Fig. 2A and C and Fig. S2A and B). These data indicated that InlB is required for efficient vacuole escape in HeLa cells.

InlB promotes Rab7 recruitment to the *Listeria*-containing vacuole (LCV). To explore the mechanism of Δ*inlB*'s delayed escape, different endosomal trafficking markers were probed over the infection time course in HeLa cells. Consistent with previous findings in macrophages (5), the key regulator of early to late endosome maturation, Rab5 (34, 35), was not found to localize to WT LCVs, and the same was observed for Δ*inlB* (Fig. S3A). A positive signal was clearly visible on control bacteria-containing vacuoles known to associate with Rab5 (*Rhodococcus equi* and *Staphylococcus aureus*) (Fig. S4A), excluding a technical issue with the antibody. Early endosomal antigen-1 (EEA1) (36) could be seen for both WT and Δ*inlB* bacteria, but only at 10 min after infection and for a small proportion of LCVs (~10%) (Fig. 3A, left, and Fig. S3B). Thus, EEA1 might have a role during the initial stages of *Listeria* endocytosis, as previously observed (25), but apparently only transient and independent of InlB.

Differences between the WT and Δ*inlB* mutant were evident, however, for the Rab7 late endosomal marker. Rab7 associated with WT LCVs soon after internalization, as previously seen in macrophages (5). The Rab7 GTPase was detected on a large proportion of phagosomes 10 min after infection, with a peak at 20 min, while it was absent 25 min later, coinciding with vacuole escape. In contrast, Δ*inlB* LCVs showed late acquisition of Rab7, with a flatter peak at 30 min followed by prolonged association up to 90 min. The phenotype could be rescued using the *inlB*-complemented mutant, indicating that it was due to InlB expression (Fig. 3A, right, and Fig. S4B). This echoed the vacuole escape experiments showing that the Δ*inlB* mutant reached the cytoplasm much later than WT (Fig. 2). Δ*inlB* was not found to colocalize with the lysosomal-associated membrane protein 1 (LAMP1), implying that although delayed in escape, the mutant was still able to avoid lysosomal fusion (Fig. S3C). Collectively, these data indicated that InlB promotes Rab7 recruitment to the LCV, and this correlated with InlB-dependent early vacuole escape.

InlB-dependent PI3P accumulation and class III PI3K (Vps34) recruitment. The phosphoinositide PI3P plays a key role in the conversion of early endosomes/phagosomes into Rab7-positive vesicles (37, 38) and was previously detected in the LCV of macrophages (5). To determine whether InlB had an effect on PI3P levels in HeLa LCVs, infection time course experiments were conducted in cells expressing a fluorescent PI3P probe (GFP-PX, consisting of the PI3P-binding PX domain from the vacuolar NADPH oxidase subunit,

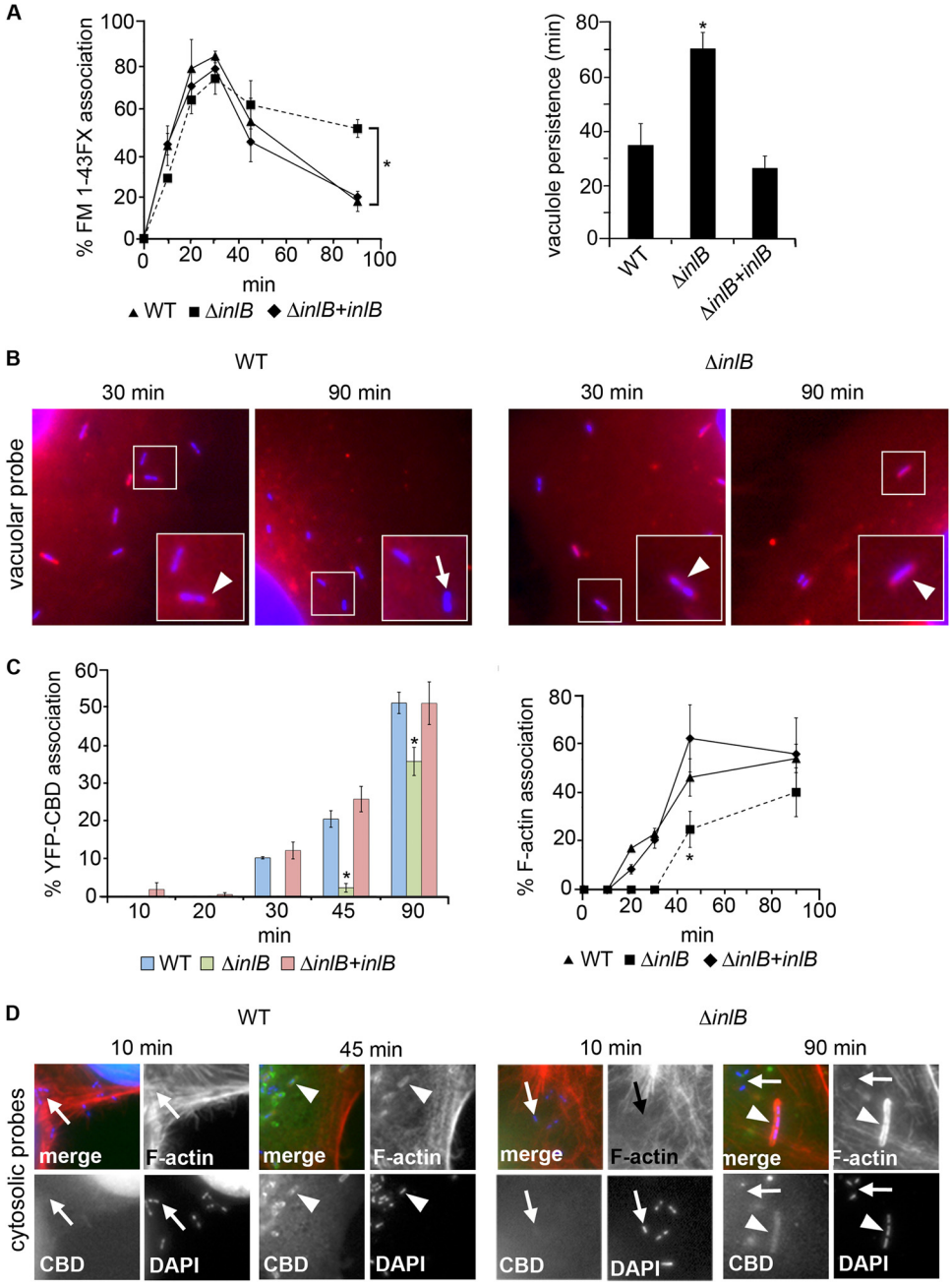

FIG 2 InlB promotes early vacuole escape. (A) (Left) Percentage of vacuole-associated WT, Δ*inlB*, and *inlB*-complemented Δ*inlB* bacteria determined using the constitutive membrane probe FM 1-43FX; (right) vacuolar persistence (VP) for each strain (see the text). *, significant difference from WT ($P < 0.01$). (B) Illustrative fluorescence micrographs for data in panel A. Shown are merged images of FM 1-43FX (phagosome membranes [red]) and DAPI (cell nuclei and bacteria [blue]) stains. Represented are ×2.5 enlarged areas of interest of images captured at ×630 magnification (see Fig. S2A for a complete image composite). The inset shows a further ×2.5 magnification of the area within the white rectangle (approximate total magnification, ×4,000). Arrowheads and arrows indicate examples of vacuolar and cytosolic bacteria, respectively. (C) Percentages of cytosolic WT, Δ*inlB*, and *inlB*-complemented Δ*inlB* bacteria as determined by decoration with CBD probe (left) or F-actin (right). *, significant difference from WT ($P < 0.01$ for 45 min on left panel and $P < 0.05$ for others). (D) Representative fluorescence micrographs for data in panel C. Shown are merged and individual channels for CBD (green), F-actin (Alexa Fluor 568-conjugated phalloidin [red]), and DAPI (bacteria and cell nuclei [blue]). Represented are ×2.5 enlarged areas of interest of images originally captured at ×630 magnification (complete image composite in Fig. S2B). Examples of YBD-CBD- and F-actin-associated and nonassociated bacteria are indicated by arrowheads and arrows, respectively.

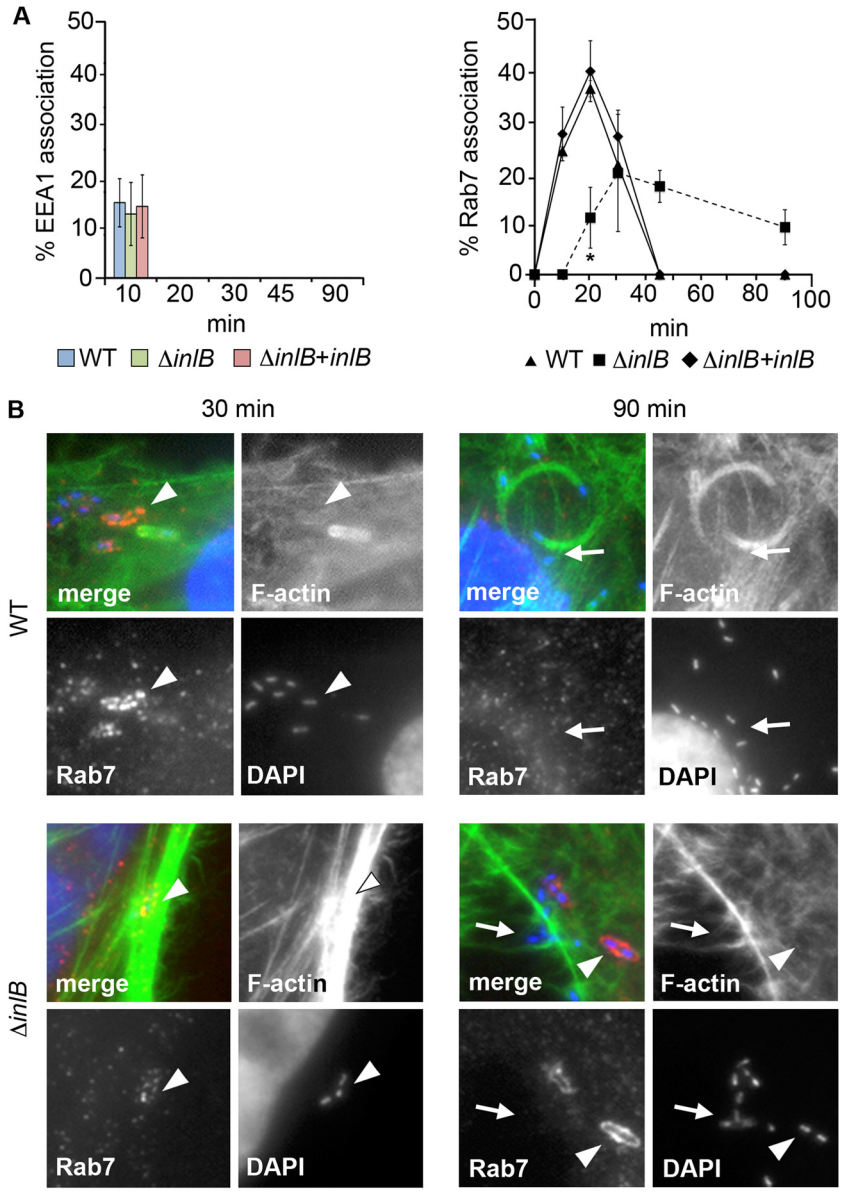

FIG 3 Transient recruitment of EEA1 and InlB-promoted accumulation of Rab7. (A) Percentage of EEA1- and Rab7-positive WT, Δ*inlB* and *inlB*-complemented Δ*inlB* LCVs. *, significant differences from WT ($P < 0.05$). (B) Representative fluorescence micrographs showing LCV association with Rab7 (for EEA1 see Fig. S3B). Shown are merged and individual channels for Rab7 (anti-Rab7 primary antibody and Alexa Fluor 568-conjugated anti-rabbit secondary antibodies [red]), F-actin (Alexa Fluor 488-conjugated phalloidin [green]), and bacteria/cell nuclei (DAPI [blue]). Shown are ×2.5 enlarged areas of interest of images originally captured at ×630 (complete image composite in Fig. S4B). Examples of Rab7-associated and nonassociated LCVs are indicated by arrowheads and arrows, respectively.

p40^{phox}, tagged with green fluorescent protein) (39). Accumulation of PI3P was observed after only 10 min in WT LCVs, with a peak by 20 min, declining by 30 min, and almost complete disappearance by 45 min after infection. In marked contrast, PI3P remained undetectable in Δ*inlB* LCVs during the 90-min time course. This again reverted to WT upon *inlB* complementation, indicating that, as for Rab7, PI3P accumulation was linked to InlB (Fig. 4A, left, Fig. 4B, and Fig. S5A). PI3P is primarily generated in endosomes and phagosomes by vacuolar protein sorting-34 (Vps34), the sole mammalian class III PI3K isoform (40, 41). Parallel experiments in which HeLa cells were stained with a Vps34 antibody showed Vps34 localizing to WT and *inlB*-complemented Δ*inlB* LCVs as early as 10 min after infection, while remaining absent from Δ*inlB* LCVs (Fig. 4A, right, Fig. 4C,

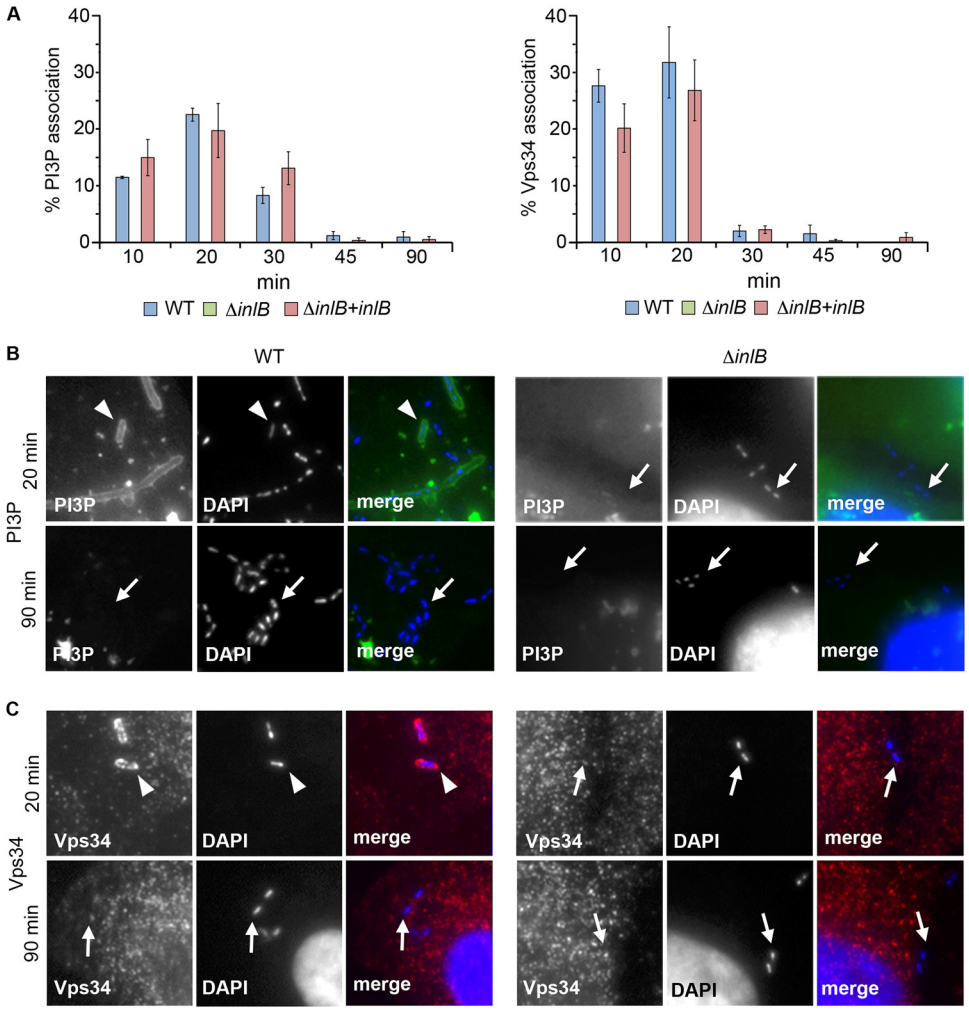

FIG 4 InlB-dependent Vps34 recruitment and PI3P accumulation. (A) Percentage of (left) PI3P (GFP-PX)-positive and (right) Vps34-positive WT, Δ*inlB* and *inlB*-complemented Δ*inlB* LCVs. (B and C) Representative single channel and merge fluorescence micrographs illustrating association with (B) the transfected PI3P-binding GFP-PX probe (green) or (C) Vps34 (monoclonal primary and Alexa Fluor 568-conjugated secondary antibodies [red]). Cell nuclei and bacteria were stained with DAPI (blue). Examples of PI3P- or Vps34-associated LCVs are indicated by arrowheads and nonassociated bacteria by arrows. See Fig. S5 for complete image composite.

Fig. S5B). This pattern mirrored the PI3P data, consistent with the absence of PI3P being due to a lack of Vps34 recruitment. Thus, the phagosomal escape deficiency caused by absence of InlB was associated with a lack of effective Vps34 recruitment and accumulation of its lipid product on the LCV.

Vps34 supports InlB-dependent intracellular proliferation but not entry. If InlB-dependent intracellular proliferation involves class III PI3K Vps34 activity, a pan-PI3K inhibitor such as wortmannin (42) should abolish it. Wortmannin treatment of preinfected HeLa cells inhibited *L. monocytogenes* intracellular proliferation to an extent similar to that seen in the absence of InlB. The effect was clearly dependent on InlB, as wortmannin did not affect the intracellular proliferation of the Δ*inlB* mutant, while significant inhibition was observed with the *inlB*- but not mock-complemented mutant (Fig. 5A, left). Wortmannin had a similar InlB-dependent inhibitory effect in Caco-2 cells and J774 macrophages (Fig. S6A).

To pinpoint the specific PI3K isoform involved, we first used isoform-specific drugs that inhibit class I PI3K. HeLa cells were treated with PIK75 (PI3Kα), TGX-221 (PI3Kβ), AS252524 (PI3Kγ) and PI-103 (PI3Kα,β,δ) (42–44), and PI3K inhibition efficacy was confirmed by Western blotting for pAktS473 (45) (Fig. S6B). None of these inhibitors

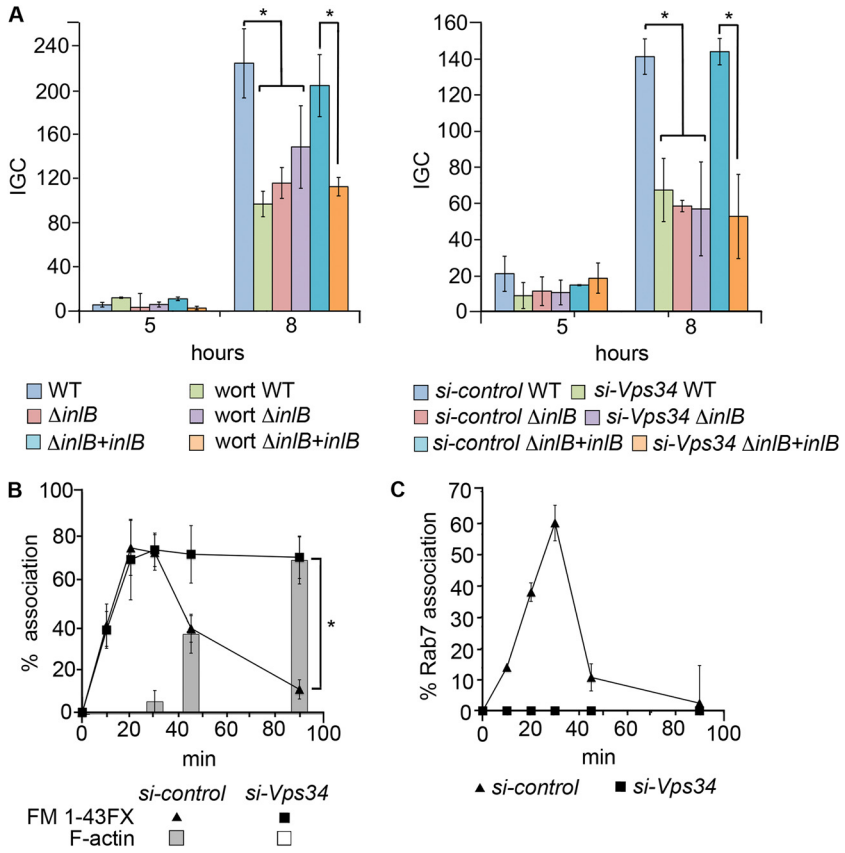

FIG 5 Vps34 supports InlB-dependent intracellular proliferation and vacuole escape. (A) Intracellular proliferation of WT, Δ*inlB*, and *inlB*-complemented Δ*inlB L. monocytogenes* in (left) wortmannin-treated HeLa cells (100 nM, nontreated cells with a corresponding amount of DMSO vehicle added; mean CFU/well at $t = 0$ [$\times 10^4$]: 3.4 ± 1.3 to 8.9 ± 3.6) or (right) cells treated with control or Vps34-specific siRNA (mean CFU/well at $t = 0$ [$\times 10^4$]: 1.7 ± 0.31 to 6.1 ± 0.47). IGC, intracellular growth coefficient. *, significant difference ($P < 0.05$). (B) Vacuole escape dynamics of *L. monocytogenes* WT in cells treated with control or Vps34-specific siRNA determined using FM 1-43FX membrane probe (vacuole-associated bacteria [line graph]) and F-actin staining (cytosolic bacteria [bars]). *, $P < 0.01$. Illustrative fluorescence micrographs are shown in Fig. S7A. (C) Same as panel B for Rab7 association (Fig. S7B).

significantly affected *Listeria* proliferation (Fig. S6C), indicating that the effect caused by wortmannin might be linked to non-class I PI3K. We next tested the involvement of class II and class III PI3K using small interfering RNA (siRNA) knockdown experiments. The siRNA treatments resulted in effective depletion of class II (PIKC2α and PIK3C2β; PIK3C2γ did not appear to be expressed in HeLa) and class III (Vps34) PI3K. Similar targeting of the class I PI3K regulatory subunit PIKR1 as a control resulted in a partial knockdown of p85 and a complete loss of class I PI3K activity as determined by pAktS473 Western blotting (Fig. S6D). Transfection with siRNA to the Met receptor required for InlB-mediated entry (17) was also used as an additional control. Both *Listeria* invasion and intracellular proliferation were investigated in the siRNA-transfected HeLa cells. While as expected (17, 24), both siPIKR1 and siMet significantly reduced cell invasion (60% and 80%, respectively), siRNAs to class II and class III PI3Ks had no effect, indicating they were not involved in the entry process (Fig. S6E). Conversely, in Vps34-, but not class I or class II PI3K-depleted cells, intracellular proliferation was significantly impaired for WT *Listeria* (Fig. 5A, right, and Fig. S6F), indicating that class III PI3K did indeed have a role in cell infection downstream entry. None of the siRNAs, including siVps34, had any effect on the already reduced intracellular proliferation of the Δ*inlB* mutant. As seen with wortmannin, complementation with *inlB* rescued the proliferation inhibition by siVps34 (Fig. 5A, right). Overall, these data indicated that Vps34 required InlB

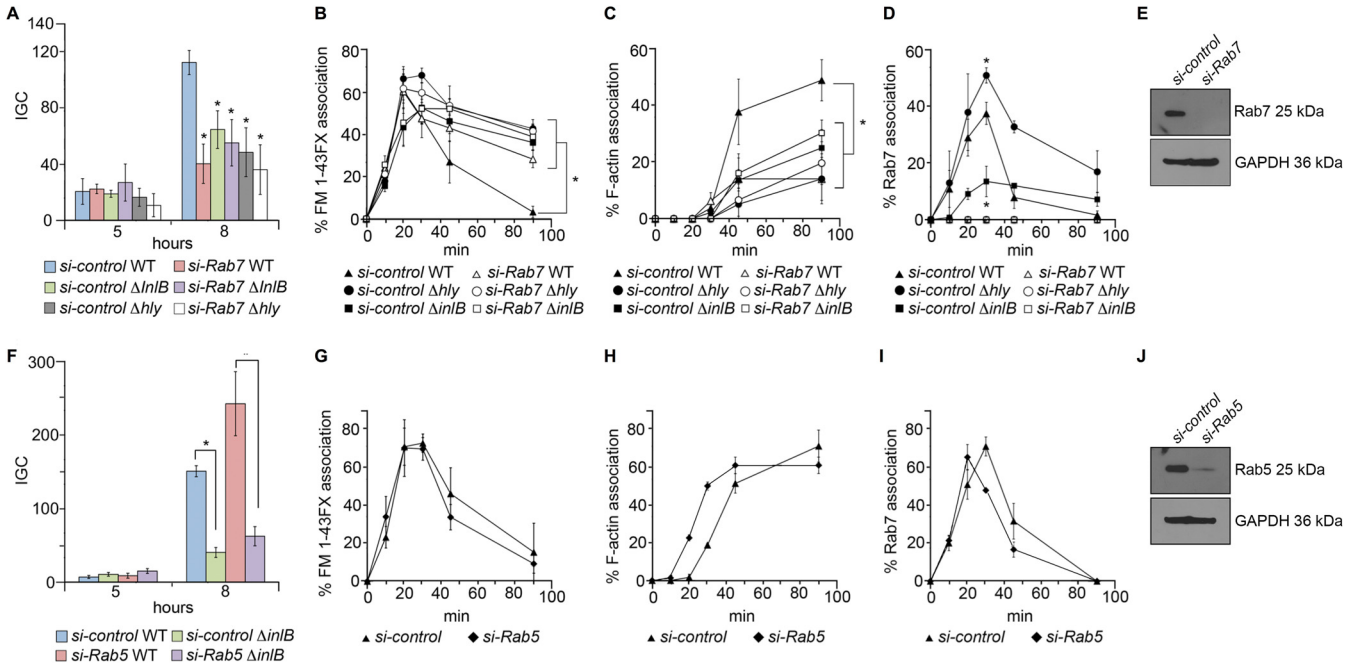

FIG 6 Rapid vacuole escape requires Rab7 and is not hindered by Rab5 inhibition in HeLa cells. (A) Intracellular proliferation of WT, Δ*inlB*, and Δ*hly* *L. monocytogenes* in Rab7-depleted or control siRNA-treated cells. IGC, intracellular growth coefficient. Mean bacterial CFU at $t = 0$ ($\times 10^4$): 2.7 ± 0.6 to 5.6 ± 1.2. *, significant difference from WT in control cells ($P < 0.05$). While capable of LLO-independent growth in HeLa cells, the early escape-defective Δ*hly* mutant (Fig. S8, left) shows significantly impaired intracellular proliferation, as seen with the Δ*inlB* mutant. (B, C, and D) Percentages of association for bacteria in panel A with membrane probe FM 1-43FX, F-actin, and Rab7. Illustrative fluorescence micrographs are shown in Fig. S8. *, significant differences ($P < 0.01$). (F) Intracellular proliferation of WT and Δ*inlB* *L. monocytogenes* in Rab5-depleted or control siRNA-treated cells. Bacterial CFU at $t = 0$ ($\times 10^4$): 3.8 ± 1.0 to 8.2 ± 1.2. *, significant differences ($P < 0.01$). (G, H, and I) Same as in panels B, C, and D for control and Rab5-depleted cells. Illustrative fluorescence micrographs are shown in Fig. S9C and D. (E and J) Depletion of Rab7 and Rab5 in siRNA-treated HeLa cells. Western immunoblotting with GAPDH was used as a loading control.

to exert its effect, suggesting that InlB and the class III PI3K act together to promote *Listeria* intracellular proliferation.

Vps34 is required for Rab7 recruitment and efficient vacuole escape. To establish whether the (InlB-dependent) effect of Vps34 on intracellular proliferation was linked to vacuole escape efficiency, siVps34- or control siRNA-treated HeLa cells were infected with WT *L. monocytogenes* and LCVs were monitored over 90 min using either FM 1-43FX or Rab7 antibody. Whereas bacteria appeared to rapidly disengage with LCVs in control cells (as determined by dissociation with the membrane probe and association with F-actin), they remained membrane associated for up to 90 min after infection in Vps34-depleted cells (Fig. 5B and Fig. S7A). Additionally, in contrast to control cells, no Rab7 could be seen around LCVs at any time point in siVps34-treated cells (Fig. 5C and Fig. S7B). These effects were essentially similar to, albeit more severe than, those observed with the *L. monocytogenes* Δ*inlB* mutant (Fig. 3A, right, and Fig. 3B), supporting the notion that InlB promotes vacuole escape by subverting LCV membrane trafficking via Vps34. These data also demonstrated the importance of Vps34 in Rab7 recruitment to the *Listeria* phagosome.

Rapid escape requires Rab7 and is not hindered by Rab5 inhibition. Listeriae appear to escape from Rab7-positive phagosomes (see reference 5 and data herein), and InlB/Vps34-promoted vacuole escape correlated with Rab7 recruitment to the LCV (this study). To test the role of Rab7 in InlB-facilitated escape, HeLa cells were transfected with control or Rab7-specific siRNAs and infected with WT or Δ*inlB* *L. monocytogenes* (Fig. 6A to E). Since the acidic pH of the maturing Rab7-positive phagosome is thought to be critical for efficient LCV disruption by LLO (5, 6), an isogenic Δ*hly* mutant was also included to determine whether Rab7 recruitment is linked to LLO-mediated escape. Although inefficiently, escape may occur in human epithelial cells in the absence of LLO, resulting in LLO-independent intracellular growth (46). We therefore verified that LLO was required for rapid vacuole escape under our conditions during the infection time course experiments in HeLa cells (Fig. 6A to D and Fig. S8A and B).

Rab7 depletion correlated with significantly reduced intracellular growth of WT *L. monocytogenes* (Fig. 6A), while it did not affect internalization (not shown). Similarly reduced intracellular growth was observed for both Δ*inlB* and Δ*hly* mutants in control cells, with no significant further change in Rab7-depleted cells (Fig. 6A). Proliferation defects correlated with significantly impaired vacuole escape, as determined by fluorescence microscopy using FM 1-43FX (Fig. 6B) and F-actin staining (Fig. 6C). As expected, Rab7 was not detected in siRab7-treated cells, while in control cells, the Rab7 acquisition pattern of WT and Δ*inlB* LCVs reproduced our previous results (Fig. 6D; see also Fig. 3A, right). No defect in Rab7 acquisition, but rather a general increase, was observed for Δ*hly* LCVs, followed by a protracted association consistent with a vacuole escape deficiency (Fig. 6D). Together, these data suggest that the effects of InlB on intracellular proliferation depend on Rab7 recruitment, in turn promoting rapid, LLO-mediated vacuole escape.

Although acquisition of the early endosomal Rab GTPase Rab5 normally precedes that of Rab7 in the endosome/phagosome maturation sequence (34, 37), Rab5 could not be recognized on HeLa (our data) or mouse macrophage (5) LCVs even immediately after infection. While this may reflect only poor or transient recruitment, evidence in macrophages suggested that Rab5 might be excluded from the LCV (5). We therefore explored in a final set of experiments the role of Rab5 in *Listeria* intracellular infection. Rab5 was inhibited in HeLa cells prior to infection either by transfection with Rab5-S34N, a dominant-negative mutant in which the GTPase is locked in GDP-bound inactive form (47), or by using an siRNA pool targeting Rab5 isoforms A, B, and C (Fig. 6J and Fig. S9A). Proliferation of WT *L. monocytogenes* was not impaired, suggesting that entry into the cytosol was not significantly affected when Rab5 function was perturbed. The defective proliferation phenotype of the Δ*inlB* mutant also remained unaffected by Rab5 inhibition (Fig. 6F and Fig. S9B). Microscopic analysis of siRNA-treated cells confirmed that vacuole escape was not delayed in Rab5-depleted cells (Fig. 6G and H). Furthermore, no interference with Rab7 recruitment was observed in siRab5-treated cells (Fig. 6I), indicating that Rab5 does not seem to play a significant role in LCV's maturation to the Rab7-positive stage.

DISCUSSION

The InlB protein is a well-known *Listeria* invasin that promotes entry into nonphagocytic cells via hijacking of the ligand-dependent Met receptor endocytic pathway and downstream activation of type I PI3K (18, 24, 25, 48). Here, we provide evidence in HeLa cells that InlB has an additional key function at later stages of intracellular infection, accelerating vacuole escape, presumably through subversion of class III PI3K signaling. InlB is sufficient to mediate this process, as shown using gene complementation analysis and pharmacological and siRNA inhibition studies. The role of InlB in LCV maturation and vacuole escape is not unique to HeLa cells as similar effects were observed in Caco-2 human enterocytes (see Fig. S10). InlB has been reported to support *Listeria* infection in epithelial cells by modulating transcriptional host cell responses via SIRT2-mediated histone H3K18 deacetylation (49). Recently, InlB-induced c-Met/class I PI3K (PI3Kα) signaling has been also found to facilitate *L. monocytogenes in vivo* persistence and invasive (e.g., brain) infection by inhibiting Fas-mediated killing of infected macrophages (50). Together with these studies, our findings highlight the growing evidence that bacterial virulence factors are multifunctional, encapsulating multiple key host-cell modulatory activities to support infection.

Cell invasion permits *Listeria* to evade extracellular host defenses while vacuolar escape is essential for intracellular survival (3, 6). Since cytosolic replication relies on successful vacuole escape, optimization of the latter by InlB maximizes listerial intracellular proliferation. *In vivo* survival also crucially depends on the ability of *L. monocytogenes* to avoid autophagy and the cytotoxic immune response directed against infected cells via a "runaway" strategy involving ActA-mediated actin-based cell-to-cell spread after cytosolic replication (3, 10). The rapid amplification of the bacterial load is clearly an essential component of this strategy because it increases the chances of

spreading before the infected cell is targeted by host defenses. Indeed, *L. monocytogenes* possesses a dedicated virulence factor to promote rapid intracellular replication, the hexose phosphate transporter Hpt (7). The vacuolar escape-accelerating activity of InlB here identified (together with its recently reported role in protecting infected monocytes from $CD8^+$-mediated killing) (50) can therefore be seen as contributing, alongside Hpt, to provide *L. monocytogenes* a competitive edge against host immunity.

Strikingly, InlB targets both extracellularly and intracellularly the endocytic pathway through interference with PI3K signaling. It seems unlikely that InlB-dependent class III PI3K (Vps34)-promoted escape is directly linked to the stimulatory effect of InlB on class I PI3K during entry because Vps34 is not known to be downstream of the Met receptor. Indeed, our data show that Vps34 supports InlB-dependent intracellular proliferation but not entry. Moreover, InlB/Vps34-promoted vacuole escape was resistant to class I PI3K isoform inhibition. Rather, these two distinct InlB functions appear to be spatiotemporally coordinated, since the hijacking of the endocytic pathway occurs at two sequential levels involving stage-specific PI3K isoforms (51) coincident with consecutive steps in *Listeria* intracellular pathogenesis. After Met/class I PI3K-mediated internalization and phagocytic cup closure, a receptor-free fraction of InlB, or InlB in complex with Met before sorting for lysosomal degradation (21, 52), might direct Vps34 recruitment to the early LCV. Cotransfection experiments demonstrated colocalization of Vps34 and PI3P in InlB-positive vesicles, but we could not detect binding between InlB and Vps34 by immunoprecipitation (data not shown). This may reflect either an interaction too weak to be captured or that InlB acts upstream of Vps34.

The catalytic subunit of class III PI3K Vps34 is an effector of the small GTPase Rab5 in the endocytic pathway and localizes to nascent endosomes in complex with several regulatory subunits through interaction with membrane-bound GTP-Rab5 (41, 51). Via Vps34, Rab5 controls recruitment of PI3P-binding proteins necessary for early endosome sorting and progression to the Rab7 late endosome stage (35, 41, 51, 53, 54). Intriguingly, however, although Vsp34 was obviously present, we could not detect Rab5 in the HeLa LCVs, recapitulating previous observations in macrophages (5). The FYVE-domain (PI3P-binding) Rab5 effector EEA1 requires not only PI3P but also corecognition by GTP-Rab5 for targeting to early endosomes (35, 51, 55). EEA1 was barely detectable in the *Listeria* phagosomes regardless of significant PI3P accumulation, consistent with Rab5 being only transiently or poorly recruited to the LCV. Indeed, in contrast to Vps34 knockdown, inhibition of Rab5 did not impede Rab7 acquisition by the LCV (or *Listeria* escape/intracellular proliferation), suggesting that Rab5 has a marginal or accessory role in the process.

Our findings do not seem to support the previous proposition that *L. monocytogenes* actively recruits and inhibits Rab5 to block LCV maturation and delay phagolysosome fusion (56, 57). Indeed, the late endosomal marker Rab7 is rapidly recruited to the LCV after *Listeria* entry in human epithelial cells (our data) and murine macrophages (5), inconsistent with phagocytic vacuole maturation being arrested. On the contrary, *L. monocytogenes* appears to expedite the process via InlB-promoted recruitment of Vps34, driving LCVs to a Rab7-positive, prelysosome (LAMP1-negative) stage. This might be facilitated by diminished Rab5 levels/EEA1-mediated fusion with other (bacterium-free, Rab5-loaded) early endosomes (34, 54, 58), as this would contribute to isolating LCVs from normal endosomal traffic. The experiments using *inlB* and *hly* mutants in Rab7-depleted cells indicated that rapid (InlB-promoted) escape takes place from Rab7-positive vacuoles and that Rab7 facilitates LLO-mediated escape, likely because of the acidified intraluminal environment of the maturing endosome (6). Consequently, InlB could be seen as acting intracellularly in concert with the low-pH-activated LLO toxin to achieve efficient vacuole escape and avoid lysosomal killing.

The apparent lack of Rab5 recruitment to the LCV is puzzling, as the coordinated replacement of Rab5 by Rab7 appears to be key in the early-to-late endosome conversion process (34, 54, 59, 60). According to the current model, upon accumulation of PI3P, the Mon1/Sand1-Ccz1 protein complex displaces the Rab5-activating guanine nucleotide

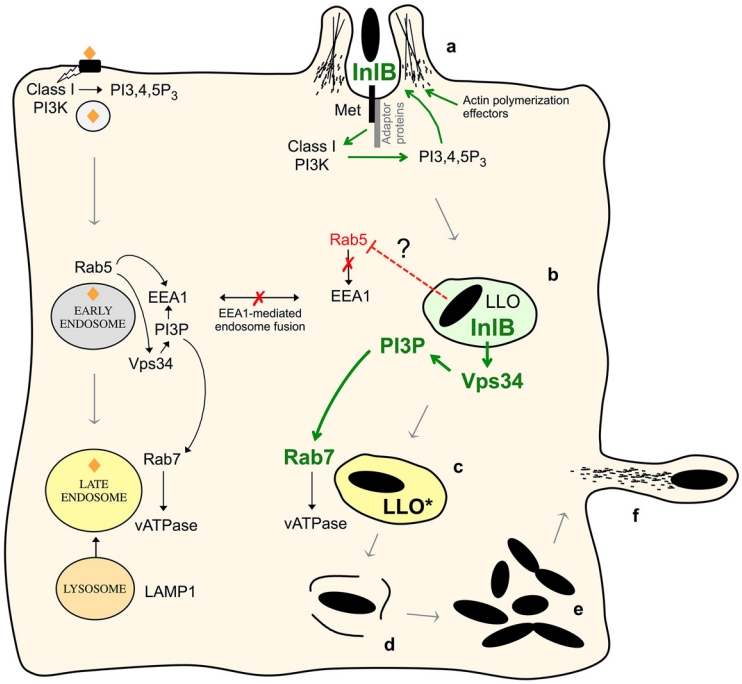

FIG 7 Model of sequential PI3K subversion by *L. monocytogenes* InlB along the endocytic pathway. At the cell surface, InlB first induces Met receptor-dependent class I PI3K activation by mimicking the natural role of HGF, leading to phagosome formation. The process involves InlB-induced autophosphorylation of the Met tyrosine kinase receptor, recruitment of adaptor proteins involved in class I PI3K recruitment/activation (Gab1, Shc, CrkII), and local accumulation of PI(3,4,5)P_3 leading to Rac1 activation, recruitment of actin polymerization promoting proteins (Ena/VASP, WAVE, N-WASP), and activation of the Arp2/3 actin-polymerizing complex (reviewed in reference 25). After entry, InlB next modulates endosomal trafficking via activation of class III PI3K (Vps34) signaling to accelerate LLO-mediated phagosome disruption, promoting intracellular bacterial survival and proliferation. Depicted on the left is the canonical endocytic pathway leading to an acidified late endosome via recruitment of the vATPase proton pump and fusion with LAMP1-positive lysosomes; on the right is depicted the "*Listeria* pathway" with the different steps of the intracellular infection cycle. (a) InlB-dependent entry. (b) Formation of a *Listeria*-containing vacuole (LCV), typically Rab5-negative, Rab7-positive, and LAMP1-negative. Lack of detection of Rab5 in the LCV, due to either defective/transient recruitment or active exclusion (5) by unknown mechanisms, impairs EEA1 acquisition and EEA1-mediated tethering and fusion with early endosomes, contributing to isolate the LCV from normal endocytic traffic. InlB bypasses the regulatory role of Rab5 in phagosome maturation by promoting the recruitment of the Rab5 downstream effector Vps34 (class III PI3K). (c) Accumulation of the Vps34 product PI3P promotes the rapid conversion of the LCV into an acidified Rab7 late endosome-like compartment in which the pore-forming toxin LLO becomes active (LLO*). (d) Vacuole disruption occurs followed by (e) rapid bacterial proliferation in the cytosol (e) and actin-based cell-to-cell spread (f). InlB-stimulated effects are indicated in green.

exchange factor (GEF) Rabex5, causing membrane dissociation of Rab5, and recruits/activates Rab7 through interaction with the HOPS (homotypic fusion and vacuole protein sorting) complex in association with the Rab7 GEF, Ccz1 (38, 54, 59, 61). Although GTP-Rab5 interacts with Mon1 and HOPS components (34, 38, 62), it is unclear whether Rab5 is strictly needed in the process once PI3P is generated by its downstream effector Vps34, because the Mon1-Ccz1 complex binds to PI3P (63, 64). Conceivably, therefore, *L. monocytogenes* might directly promote Rab7 accumulation without a sustained Rab5 input via InlB-modulated Vps34 recruitment and concomitant PI3P generation (Fig. 7). It is worth noting, however, that even in the absence of InlB, and thus of detectable Vps34 and PI3P accumulation, Rab7 acquisition still occurred in the LCV, albeit more slowly. This observation is consistent with previous data showing significant Rab7 recruitment to phagosomes in wortmannin-treated cells (37), implying that the phagosome maturation process can be, at least partially, independent of Vps34 activity (65). Nevertheless, our siRNA experiments support a crucial role for Vps34 because its depletion appeared to prevent Rab7 recruitment to the LCV. Since via a regulatory loop Vps34 negatively regulates Rab5 during endosome maturation (66), InlB-promoted Vps34 recruitment itself might have a role in the lack

of detection of Rab5 in the LCV. Multiple mediators and interactors are involved in the intricate regulation of endosome trafficking (41, 51, 54, 59, 60), and further research is needed to clarify the mechanism underlying the apparent Rab5 exclusion and how InlB promotes Vps34 and Rab7 recruitment in the LCV.

Avoidance of lysosomal killing by vacuolar pathogens often involves interference with class III PI3K/PI3P signaling, but the specific underlying mechanism differs for each pathogen (67, 68). *M. tuberculosis*, for example, causes early phagosome maturation arrest through depletion of PI3P by the secreted SapM phosphatase as well as inhibition of Vps34 by mycobacterial cell envelope components. Rab5 is retained, but EEA1 and Rab7 are excluded, blocking acquisition of the acidifying vacuolar proton pump ATPase and lysosomal fusion (69–72). *Salmonella*, in contrast, promotes homotypic fusion of PI3P-enriched, Rab5- and EEA1-positive vesicles to form a large vacuole in which the bacteria proliferate. This is mediated by the type III secreted effector SopB, which promotes PI3P generation by dephosphorylating phosphatidylinositol di- and triphosphates and through recruitment of Rab5 and Vps34 activation (73, 74). Here, we show that *L. monocytogenes*, via InlB, promotes the recruitment of Vps34 and induces PI3P generation on the LCV, boosting the formation of an escape-favorable Rab7 late phagosome. Our data offer a novel example of bacterial modulation of endosomal trafficking, unexpectedly in a cytosolically replicating pathogen that only very transiently interacts with the phagocytic vacuole after internalization.

MATERIALS AND METHODS

Bacteria, plasmids, antibodies, and reagents. Isogenic derivatives of *L. monocytogenes* serovar 4b clinical isolate P14 with constitutive *in vivo*-like virulence gene expression (75) were used in this study. The construction of Δ*inlA* and Δ*inlB* in-frame deletion mutants is described below, the Δ*actA* and Δ*hly* mutants have been reported elsewhere (27, 76). The *R. equi* 103S and *S. aureus* USA300 strains used as controls for Rab5 detection in bacterial phagosomes were from our bacterial isolate collection and R. Fitzgerald's laboratory (Roslin Institute, University of Edinburgh), respectively. Mammalian expression plasmids pEYFP-CBD, encoding the *Listeria* cell wall-binding cytosolic probe, and pGFP-iPX, encoding the PI3P-binding probe, were kindly provided by J. Swanson's lab (University of Michigan Medical School, Ann Arbor, MI, USA) and the L. Stephen/P. Hawkins's lab (Babraham Institute, Cambridge, United Kingdom), respectively (5, 39). The plasmid pHinlB used for complementation of the Δ*inlB* mutant is a derivative of the *E. coli* Gram-positive shuttle vector pHPS9 (77) containing the *inlB* gene. The insert was prepared by PCR amplification of *inlB* and upstream *inlAB* operon regulatory regions from *L. monocytogenes* PAM14 Δ*inlA* genomic DNA using oligonucleotides mainI13SalI13 (ACGCGTCGACGAACATAAAGGGTAGAGG) and inlBBamHI (CGGGATCCCGATTCTTGCTAGACCACC), which carry SalI and BamHI restriction sites (underlined), respectively. After cloning into the pTOPO cloning T-vector (Invitrogen), the SalI/BamHI insert was transferred to pHPS9.

Reagents, antibodies, and oligonucleotides. Chemicals were from Sigma-Aldrich unless stated otherwise. Class I PI3K inhibitors PIK-75, TGX-221, AS-604850, and PI-103 were from Cayman Chemicals. FM 1-43FX membrane probe was from Life Technologies. Antibodies to Akt, pAktS473, Rab7, Rab5, EEA1, and Vps34 were from Cell Signaling Technology, GAPDH (glyceraldehyde-3-phosphate dehydrogenase) from Chemicon, p85 from Millipore, PI3KC2α and PI3KC2β from BD Biosciences, PI3KC2γ from Abgent, LAMP1 (H4A3) from Santa Cruz, and horseradish peroxidase (HRP)-conjugated-mouse and rabbit antibodies from Amersham. Specific antibodies to InlA and InlB were kindly provided by P. Cossart, Institut Pasteur, Paris, France. Oligonucleotides for siRNA knockdowns were from Dharmacon. Pools of four individual siRNA oligonucleotides were used to target each of the human PI3K genes PIK3R1 (D-003020-10, D-003020-11, D-003020-26, D-003020-27) PIK2CA (D-006677-01, D-006771-02, D-006771-03, D-006771-04), PIK2CB (D-006772-01, D-006772-02, D-006772-03, D-006772-04), PIK2CG (D-006773-01, D-006773-02, D-006773-03, D-006773-04) and PIK3C3 (D-005250-01, D-005250-02, D-005250-03, D-005250-04). Pools of four oligonucleotides were also used for Rab5A (D-004009-01, D-004009-02, D-004009-03 D-004009-04), Rab5B (D-004010-1, D-004010-2, D-004010-3, D-004010-4), Rab5C (D-004011-1, D-004011-2, D-004011-3, D-004011-4), and Rab7 (D-010388-01, D-010388-02, D-010388-03, D-010388-04), while the HGF receptor Met was targeted with oligonucleotide D-003156-13. Oligonucleotide primers for PCR or genetic constructs were purchased from Sigma or Metabion (Martinsried, Germany).

General DNA techniques. Restriction enzymes were used according to the manufacturer's instructions (Promega and NEB). Chromosomal DNA from *Listeria* was extracted and purified as previously described (75). Plasmid DNA was extracted from *E. coli* using the Qiagen plasmid purification kit and was introduced into *E. coli* or *L. monocytogenes* by electroporation using a GenePulserXcell apparatus (Bio-Rad). PCR was carried out with *Taq* DNA polymerase (Biotools, Madrid, Spain) for detection/mapping purposes or high-fidelity ProofStart DNA polymerase (Qiagen) for plasmid or mutant constructions. The reaction mixtures contained 100 ng of DNA template, 200 μM deoxynucleoside triphosphates (dNTPs), 0.25 μg oligonucleotide primers, 2.5 mM $MgCl_2$, a suitable amount of polymerase buffer, and 1 U of polymerase per kb in a 25-μL volume. The standard amplification program was 3 min at 94°C, followed by 30 cycles of 15 s at 95°C, 30 to 60 s at 48 to 58°C, and 1 to 3 min at 72°C, and a final 3 min at

72°C. PCR products were purified with the Qiagen PCR purification kit. DNA sequences were determined on both strands.

Construction of *L. monocytogenes inlA* and *inlB* in-frame deletion mutants. Chromosomal gene deletions were generated by allelic exchange via homologous recombination as previously described (76). For the Δ*inlA* mutant, the recombinogenic plasmid was constructed by in-frame ligation of two PCR fragments containing small portions of the 5′- and 3′-terminal regions of the *inlA* gene plus part of the upstream and downstream flanking regions, respectively. Oligonucleotides inlA1 (ATTTGGATCCTAAAG GGTAGAGG) and inlA2 (CATACCCCGGGGCCAAATACT) carrying BamHI and XmaI/SmaI sites, respectively (underlined), were used to PCR amplify a 643-bp fragment from the 5′ region of *inlA*, including the first 72 bp of the gene. Similarly, oligonucleotides inlA3 (TCACCCGGGAATTCAGCTAGC) and inlA4 (TGAACGG ATCCAATATCACTATTAT) carrying XmaI/SmaI and BamHI sites, respectively, were used to amplify a 709-bp fragment from the 3′ region of *inlA*, including the last 174 nucleotides of the gene. The two PCR products were digested with XmaI and ligated, and the ligation product was used as a template for PCR amplification with oligonucleotides inlA1 and inlA4. The resulting amplicon was inserted into the pTOPO T-vector (Invitrogen) and then the BamHI fragment containing the Δ*inlA* construct was transferred to the thermosensitive shuttle vector pMAD (78) to give the recombinogenic plasmid pMΔ*inlA*. The in-frame-deleted allele for the Δ*inlB* mutant was generated by "recombinant PCR" (79). Oligonucleotide primers inlB1 (TCCTGTGGATCCACCAACAACT) and inlB2R (TACCGGAACTTTTGTCACTAGATCCGTCACAC) amplified a 573-bp fragment from the 5′ region of *inlB*, including the first 213 bp of the gene, and primers inlB3R (GATCTAGTGACAAAGTTCCGGTAGTAGATAGC) and inlB4 (GTGATGGATCCCACATTTTGGC) were used to amplify the 3′ region of *inlB*. Primers inlB1 and inlB4 carried BamHI sites, and primers inlB2R and inlB3R had complementary sequences (underlined). The two PCR products were fused by splicing overlap extension using oligonucleotides inlB1 and inlB4, and the recombinant PCR product was processed as described above to produce the pMAD-based recombinogenic plasmid pMΔ*inlB*.

Mammalian cell cultures and transfections. HeLa cells (and Caco-2 and J774 cells for some control experiments) were sourced from ATCC, passaged at no more than 70% confluence, and used between passages 3 and 15. Cells were cultured in 24-well plates or on 13-mm glass coverslips at 37°C under 5% CO_2 in DMEM (Dulbecco's modified Eagle's medium supplemented with 10% fetal calf serum [FCS] and L-glutamine [Invitrogen]) without antibiotics, as previously described (45). HeLa cells were seeded at a density of 3.5×10^4 or 5×10^4 cells per well (24-well plates) or coverslip 24 h prior to transfection with siRNA or plasmid, respectively. Plasmid DNA or siRNAs diluted in optiMEM without FCS were premixed with optiMEM-diluted Lipofectamine 2000 reagent (Invitrogen) as per the manufacturer's instructions. Cells were transfected for 12 h in 1 mL DMEM, giving a final concentration of 80 to 200 nM oligonucleotide or 1 to 5 μg/mL plasmid DNA. Transfected cells were incubated for 24 h prior to infection, fixation for immunofluorescence microscopy, or production of cell lysates. Plasmid transfection efficiency was typically >85%.

Cell infections. Culture plates containing $\approx 1 \times 10^5$ cells per well were inoculated with bacterial suspensions in DMEM and immediately centrifuged ($180 \times g$, 3 min) to synchronize infection. Internalization and intracellular proliferation assays were carried out using a gentamicin protection assay as previously described (27). After centrifugation, inoculated plates were incubated for 30 min (15 min for J774 macrophages) and washed several times with Dulbecco's phosphate-buffered saline (DPBS) (Invitrogen) followed by a further incubation in DMEM containing 100 μg/mL gentamicin for 30 min to kill the remaining extracellular bacteria. Samples were taken at this point to determine invasion ($t = 0$), and medium was replaced with fresh medium containing 10 μg/mL gentamicin to prevent extracellular bacterial growth. Where applicable, PI3K inhibitors were added at this stage diluted in 0.1% dimethyl sulfoxide (DMSO). At the sampling time points, cells were washed in DPBS, lysed in 10 mM Tris-HCl (pH 7.4), 1% Triton X-100, and viable bacteria plate counted. Intracellular proliferation data were normalized using an intracellular growth coefficient to correct for variation in cell entry using the formula $IGC = (CFU_{tn} - CFU_{t0})/CFU_{t0}$ (27).

Western blotting. HeLa cells were processed for immunoblotting as detailed by Cain et al. (45), and bacterial proteins were prepared as previously described (76). Immunoreactive proteins were visualized using the ECL enhanced chemiluminescence detection system (Amersham).

Fluorescence microscopy. Coverslips for time course quantifications were collected 10, 20, 30, 45, and 90 min after plate centrifugation, thoroughly washed four times in warm PBS to remove extracellular bacteria, fixed with 3.7% (wt/vol) paraformaldehyde, and processed as described by Cain et al. (45). For time points 45 and 90 min, 100 μg/mL gentamicin was added to the medium 30 min after infection to prevent extracellular growth. Alexa Fluor 488- or 568-conjugated anti-rabbit or anti-mouse IgG secondary antibodies (1 h) were used for immunofluorescence staining, followed by Alexa Fluor 568- or 488-conjugated phalloidin (Invitrogen) and DAPI (4′,6-diamidino-2-phenylindole) (Sigma) (20 min) to visualize F-actin and bacterial DNA/cell nuclei, respectively. To determine vacuole-associated bacteria, cells were incubated with 2 μM of the fixable fluorescent membrane probe FM 1-43FX (Life Technologies) in DMEM for 45 min, washed twice, and incubated with fresh DMEM for 30 min before infection. Bacteria that escaped from the vacuole were identified based on their association with either F-actin (46) or a transfected listerial cell wall-binding fluorescent cytosolic probe (yellow fluorescent protein [YFP]-CBD) (5). Images were acquired at room temperature using a Leica CTR-6000 fluorescence microscope with a 63× oil immersion objective, collecting data as a z-stack, which were later flattened by deconvolution. Images were processed using Leica LAF software (Leica) and ImageJ (NIH; http://rsbweb.nih.gov/ij/), and figures were assembled using Adobe Photoshop.

Statistics. In all cases, data are shown as the mean ± standard error of the mean (SEM) of values from a minimum of three independent experiments performed in triplicate. Data for image-based quantifications were collected from 60 to 70 bacteria/vacuoles across five randomly selected microscopic

fields per time point per condition in each of three independent experiments. The statistical significance of data was determined by Student *t* tests using Prism software (http://www.graphpad.com/scientific-software/prism/).

SUPPLEMENTAL MATERIAL

Supplemental material is available online only.

FIG S1, TIF file, 0.9 MB.

FIG S2, TIF file, 2.6 MB.

FIG S3, TIF file, 2.6 MB.

FIG S4, TIF file, 2.7 MB.

FIG S5, TIF file, 2.6 MB.

FIG S6, TIF file, 1.3 MB.

FIG S7, TIF file, 2.8 MB.

FIG S8, TIF file, 2.9 MB.

FIG S9, TIF file, 2.6 MB.

FIG S10, TIF file, 2.8 MB.

ACKNOWLEDGMENTS

We thank J. Swanson for kindly providing the CBD probe, P. Hawkins for the pGFP-iPX plasmid, R. Fitzgerald for the *S. aureus* US300 strain, and P. Cossart and E. Gouin for InlA and InlB antibodies.

This work was funded by the Wellcome Trust (program grant WT074020MA to J.V.-B).

REFERENCES

1. Koopmans MM, Brouwer MC, Vázquez-Boland JA, van de Beek D. 2022. Human listeriosis. Clin Microbiol Rev https://doi.org/10.1128/cmr.00060-19.
2. Cossart P. 2011. Illuminating the landscape of host-pathogen interactions with the bacterium *Listeria monocytogenes*. Proc Natl Acad Sci U S A 108:19484–19491. https://doi.org/10.1073/pnas.1112371108.
3. Ray K, Marteyn B, Sansonetti PJ, Tang CM. 2009. Life on the inside: the intracellular lifestyle of cytosolic bacteria. Nat Rev Microbiol 7:333–340. https://doi.org/10.1038/nrmicro2112.
4. Beauregard KE, Lee KD, Collier RJ, Swanson JA. 1997. pH-dependent perforation of macrophage phagosomes by listeriolysin O from *Listeria monocytogenes*. J Exp Med 186:1159–1163. https://doi.org/10.1084/jem.186.7.1159.
5. Henry R, Shaughnessy L, Loessner MJ, Alberti-Segui C, Higgins DE, Swanson JA. 2006. Cytolysin-dependent delay of vacuole maturation in macrophages infected with *Listeria monocytogenes*. Cell Microbiol 8:107–119. https://doi.org/10.1111/j.1462-5822.2005.00604.x.
6. Schnupf P, Portnoy DA. 2007. Listeriolysin O: a phagosome-specific lysin. Microbes Infect 9:1176–1187. https://doi.org/10.1016/j.micinf.2007.05.005.
7. Chico-Calero I, Suarez M, Gonzalez-Zorn B, Scortti M, Slaghuis J, Goebel W, Vazquez-Boland JA, European Listeria Genome Consortium. 2002. Hpt, a bacterial homolog of the microsomal glucose-6-phosphate translocase, mediates rapid intracellular proliferation in *Listeria*. Proc Natl Acad Sci U S A 99:431–436. https://doi.org/10.1073/pnas.012363899.
8. Kocks C, Gouin E, Tabouret M, Berche P, Ohayon H, Cossart P. 1992. *L. monocytogenes*-induced actin assembly requires the *actA* gene product, a surface protein. Cell 68:521–531. https://doi.org/10.1016/0092-8674(92)90188-i.
9. Birmingham CL, Canadien V, Gouin E, Troy EB, Yoshimori T, Cossart P, Higgins DE, Brumell JH. 2007. *Listeria monocytogenes* evades killing by autophagy during colonization of host cells. Autophagy 3:442–451. https://doi.org/10.4161/auto.4450.
10. Portnoy DA, Auerbuch V, Glomski IJ. 2002. The cell biology of *Listeria monocytogenes* infection: the intersection of bacterial pathogenesis and cell-mediated immunity. J Cell Biol 158:409–414. https://doi.org/10.1083/jcb.200205009.
11. Bierne H, Sabet C, Personnic N, Cossart P. 2007. Internalins: a complex family of leucine-rich repeat-containing proteins in *Listeria monocytogenes*. Microbes Infect 9:1156–1166. https://doi.org/10.1016/j.micinf.2007.05.003.
12. Rajabian T, Gavicherla B, Heisig M, Muller-Altrock S, Goebel W, Gray-Owen SD, Ireton K. 2009. The bacterial virulence factor InlC perturbs apical cell junctions and promotes cell-to-cell spread of *Listeria*. Nat Cell Biol 11:1212–1218. https://doi.org/10.1038/ncb1964.
13. Gouin E, Adib-Conquy M, Balestrino D, Nahori MA, Villiers V, Colland F, Dramsi S, Dussurget O, Cossart P. 2010. The *Listeria monocytogenes* InlC protein interferes with innate immune responses by targeting the IκB kinase subunit IKKα. Proc Natl Acad Sci U S A 107:17333–17338. https://doi.org/10.1073/pnas.1007765107.
14. Gaillard JL, Berche P, Frehel C, Gouin E, Cossart P. 1991. Entry of *L. monocytogenes* into cells is mediated by internalin, a repeat protein reminiscent of surface antigens from Gram-positive cocci. Cell 65:1127–1141. https://doi.org/10.1016/0092-8674(91)90009-n.
15. Mengaud J, Ohayon H, Gounon P, Mege RM, Cossart P. 1996. E-cadherin is the receptor for internalin, a surface protein required for entry of *L. monocytogenes* into epithelial cells. Cell 84:923–932. https://doi.org/10.1016/s0092-8674(00)81070-3.
16. Schubert WD, Urbanke C, Ziehm T, Beier V, Machner MP, Domann E, Wehland J, Chakraborty T, Heinz DW. 2002. Structure of internalin, a major invasion protein of *Listeria monocytogenes*, in complex with its human receptor E-cadherin. Cell 111:825–836. https://doi.org/10.1016/S0092-8674(02)01136-4.
17. Shen Y, Naujokas M, Park M, Ireton K. 2000. InlB-dependent internalization of *Listeria* is mediated by the Met receptor tyrosine kinase. Cell 103:501–510. https://doi.org/10.1016/s0092-8674(00)00141-0.
18. Niemann HH, Jager V, Butler PJ, van den Heuvel J, Schmidt S, Ferraris D, Gherardi E, Heinz DW. 2007. Structure of the human receptor tyrosine kinase met in complex with the *Listeria* invasion protein InlB. Cell 130:235–246. https://doi.org/10.1016/j.cell.2007.05.037.
19. Disson O, Grayo S, Huillet E, Nikitas G, Langa-Vives F, Dussurget O, Ragon M, Le Monnier A, Babinet C, Cossart P, Lecuit M. 2008. Conjugated action of two species-specific invasion proteins for fetoplacental listeriosis. Nature 455:1114–1118. https://doi.org/10.1038/nature07303.
20. Pentecost M, Kumaran J, Ghosh P, Amieva MR. 2010. *Listeria monocytogenes* internalin B activates junctional endocytosis to accelerate intestinal invasion. PLoS Pathog 6:e1000900. https://doi.org/10.1371/journal.ppat.1000900.
21. Veiga E, Cossart P. 2005. *Listeria* hijacks the clathrin-dependent endocytic machinery to invade mammalian cells. Nat Cell Biol 7:894–900. https://doi.org/10.1038/ncb1292.
22. Bonazzi M, Veiga E, Pizarro-Cerda J, Cossart P. 2008. Successive post-translational modifications of E-cadherin are required for InlA-mediated internalization of *Listeria monocytogenes*. Cell Microbiol 10:2208–2222. https://doi.org/10.1111/j.1462-5822.2008.01200.x.

23. Bonazzi M, Vasudevan L, Mallet A, Sachse M, Sartori A, Prevost MC, Roberts A, Taner SB, Wilbur JD, Brodsky FM, Cossart P. 2011. Clathrin phosphorylation is required for actin recruitment at sites of bacterial adhesion and internalization. J Cell Biol 195:525–536. https://doi.org/10.1083/jcb.201105152.
24. Ireton K, Payrastre B, Cossart P. 1999. The *Listeria monocytogenes* protein InlB is an agonist of mammalian phosphoinositide 3-kinase. J Biol Chem 274:17025–17032. https://doi.org/10.1074/jbc.274.24.17025.
25. Pizarro-Cerda J, Cossart P. 2018. *Listeria monocytogenes*: cell biology of invasion and intracellular growth. Microbiol Spectr https://doi.org/10.1128/microbiolspec.GPP3-0013-2018.
26. de las Heras A, Cain RJ, Bielecka MK, Vazquez-Boland JA. 2011. Regulation of *Listeria* virulence: PrfA master and commander. Curr Opin Microbiol 14:118–127. https://doi.org/10.1016/j.mib.2011.01.005.
27. Deshayes C, Bielecka MK, Cain RJ, Scortti M, de las Heras A, Pietras Z, Luisi BF, Nunez Miguel R, Vazquez-Boland JA. 2012. Allosteric mutants show that PrfA activation is dispensable for vacuole escape but required for efficient spread and *Listeria* survival *in vivo*. Mol Microbiol 85:461–477. https://doi.org/10.1111/j.1365-2958.2012.08121.x.
28. Milohanic E, Glaser P, Coppee JY, Frangeul L, Vega Y, Vazquez-Boland JA, Kunst F, Cossart P, Buchrieser C. 2003. Transcriptome analysis of *Listeria monocytogenes* identifies three groups of genes differently regulated by PrfA. Mol Microbiol 47:1613–1625. https://doi.org/10.1046/j.1365-2958.2003.03413.x.
29. Chatterjee SS, Hossain H, Otten S, Kuenne C, Kuchmina K, Machata S, Domann E, Chakraborty T, Hain T. 2006. Intracellular gene expression profile of *Listeria monocytogenes*. Infect Immun 74:1323–1338. https://doi.org/10.1128/IAI.74.2.1323-1338.2006.
30. Joseph B, Przybilla K, Stuhler C, Schauer K, Slaghuis J, Fuchs TM, Goebel W. 2006. Identification of *Listeria monocytogenes* genes contributing to intracellular replication by expression profiling and mutant screening. J Bacteriol 188:556–568. https://doi.org/10.1128/JB.188.2.556-568.2006.
31. Gregory SH, Sagnimeni AJ, Wing EJ. 1997. Internalin B promotes the replication of *Listeria monocytogenes* in mouse hepatocytes. Infect Immun 65:5137–5141. https://doi.org/10.1128/iai.65.12.5137-5141.1997.
32. Bauer S, Tapper H. 2004. Membrane retrieval in neutrophils during phagocytosis: inhibition by M protein-expressing *S. pyogenes* bacteria. J Leukoc Biol 76:1142–1150. https://doi.org/10.1189/jlb.0404260.
33. Bertrand CA, Laboisse C, Hopfer U, Bridges RJ, Frizzell RA. 2006. Methods for detecting internalized, FM 1-43 stained particles in epithelial cells and monolayers. Biophys J 91:3872–3883. https://doi.org/10.1529/biophysj.106.086983.
34. Rink J, Ghigo E, Kalaidzidis Y, Zerial M. 2005. Rab conversion as a mechanism of progression from early to late endosomes. Cell 122:735–749. https://doi.org/10.1016/j.cell.2005.06.043.
35. Grosshans BL, Ortiz D, Novick P. 2006. Rabs and their effectors: achieving specificity in membrane traffic. Proc Natl Acad Sci U S A 103:11821–11827. https://doi.org/10.1073/pnas.0601617103.
36. Simonsen A, Lippe R, Christoforidis S, Gaullier JM, Brech A, Callaghan J, Toh BH, Murphy C, Zerial M, Stenmark H. 1998. EEA1 links PI(3)K function to Rab5 regulation of endosome fusion. Nature 394:494–498. https://doi.org/10.1038/28879.
37. Vieira OV, Bucci C, Harrison RE, Trimble WS, Lanzetti L, Gruenberg J, Schreiber AD, Stahl PD, Grinstein S. 2003. Modulation of Rab5 and Rab7 recruitment to phagosomes by phosphatidylinositol 3-kinase. Mol Cell Biol 23:2501–2514. https://doi.org/10.1128/MCB.23.7.2501-2514.2003.
38. Poteryaev D, Datta S, Ackema K, Zerial M, Spang A. 2010. Identification of the switch in early-to-late endosome transition. Cell 141:497–508. https://doi.org/10.1016/j.cell.2010.03.011.
39. Ellson C, Davidson K, Anderson K, Stephens LR, Hawkins PT. 2006. PtdIns3P binding to the PX domain of p40phox is a physiological signal in NADPH oxidase activation. EMBO J 25:4468–4478. https://doi.org/10.1038/sj.emboj.7601346.
40. Vieira OV, Botelho RJ, Rameh L, Brachmann SM, Matsuo T, Davidson HW, Schreiber A, Backer JM, Cantley LC, Grinstein S. 2001. Distinct roles of class I and class III phosphatidylinositol 3-kinases in phagosome formation and maturation. J Cell Biol 155:19–25. https://doi.org/10.1083/jcb.200107069.
41. Backer JM. 2016. The intricate regulation and complex functions of the class III phosphoinositide 3-kinase Vps34. Biochem J 473:2251–2271. https://doi.org/10.1042/BCJ20160170.
42. Knight ZA, Gonzalez B, Feldman ME, Zunder ER, Goldenberg DD, Williams O, Loewith R, Stokoe D, Balla A, Toth B, Balla T, Weiss W, Williams RL, Shokat KM. 2006. A pharmacological map of the PI3-K family defines a role for p110α in insulin signaling. Cell 125:733–747. https://doi.org/10.1016/j.cell.2006.03.035.
43. Camps M, Ruckle T, Ji H, Ardissone V, Rintelen F, Shaw J, Ferrandi C, Chabert C, Gillieron C, Francon B, Martin T, Gretener D, Perrin D, Leroy D, Vitte PA, Hirsch E, Wymann MP, Cirillo R, Schwarz MK, Rommel C. 2005. Blockade of PI3Kγ suppresses joint inflammation and damage in mouse models of rheumatoid arthritis. Nat Med 11:936–943. https://doi.org/10.1038/nm1284.
44. Jackson SP, Schoenwaelder SM, Goncalves I, Nesbitt WS, Yap CL, Wright CE, Kenche V, Anderson KE, Dopheide SM, Yuan Y, Sturgeon SA, Prabaharan H, Thompson PE, Smith GD, Shepherd PR, Daniele N, Kulkarni S, Abbott B, Saylik D, Jones C, Lu L, Giuliano S, Hughan SC, Angus JA, Robertson AD, Salem HH. 2005. PI 3-kinase p110β: a new target for antithrombotic therapy. Nat Med 11:507–514. https://doi.org/10.1038/nm1232.
45. Cain RJ, Vanhaesebroeck B, Ridley AJ. 2010. The PI3K p110alpha isoform regulates endothelial adherens junctions via Pyk2 and Rac1. J Cell Biol 188:863–876. https://doi.org/10.1083/jcb.200907135.
46. Marquis H, Doshi V, Portnoy D. 1995. The broad range phospholipase C and a metalloprotease mediated listeriolysin O-independent escape of *Listeria monocytogenes* from a primary vacuole in human epithelial cells. Infect Immun 63:4531–4534. https://doi.org/10.1128/iai.63.11.4531-4534.1995.
47. Li G, Stahl PD. 1993. Structure-function relationship of the small GTPase rab5. J Biol Chem 268:24475–24480. https://doi.org/10.1016/S0021-9258(20)80550-X.
48. Banerjee M, Copp J, Vuga D, Marino M, Chapman T, van der Geer P, Ghosh P. 2004. GW domains of the *Listeria monocytogenes* invasion protein InlB are required for potentiation of Met activation. Mol Microbiol 52:257–271. https://doi.org/10.1111/j.1365-2958.2003.03968.x.
49. Eskandarian HA, Impens F, Nahori M-A, Soubigou G, Coppée J-Y, Cossart P, Hamon MA. 2013. A role for SIRT2-dependent histone H3K18 deacetylation in bacterial infection. Science 341:1238858. https://doi.org/10.1126/science.1238858.
50. Maudet C, Kheloufi M, Levallois S, Gaillard J, Huang L, Gaultier C, Tsai Y-H, Disson O, Lecuit M. 2022. Bacterial inhibition of Fas-mediated killing promotes neuroinvasion and persistence. Nature 603:900–906. https://doi.org/10.1038/s41586-022-04505-7.
51. Bilanges B, Posor Y, Vanhaesebroeck B. 2019. PI3K isoforms in cell signalling and vesicle trafficking. Nat Rev Mol Cell Biol 20:515–534. https://doi.org/10.1038/s41580-019-0129-z.
52. Lefebvre J, Ancot F, Leroy C, Muharram G, Lemiere A, Tulasne D. 2012. Met degradation: more than one stone to shoot a receptor down. FASEB J 26:1387–1399. https://doi.org/10.1096/fj.11-197723.
53. Kinchen JM, Ravichandran KS. 2008. Phagosome maturation: going through the acid test. Nat Rev Mol Cell Biol 9:781–795. https://doi.org/10.1038/nrm2515.
54. Wandinger-Ness A, Zerial M. 2014. Rab proteins and the compartmentalization of the endosomal system. Cold Spring Harb Perspect Biol 6:a022616. https://doi.org/10.1101/cshperspect.a022616.
55. Mishra A, Eathiraj S, Corvera S, Lambright DG. 2010. Structural basis for Rab GTPase recognition and endosome tethering by the C_2H_2 zinc finger of Early Endosomal Autoantigen 1 (EEA1). Proc Natl Acad Sci U S A 107:10866–10871. https://doi.org/10.1073/pnas.1000843107.
56. Alvarez-Dominguez C, Roberts R, Stahl PD. 1997. Internalized *Listeria monocytogenes* modulates intracellular trafficking and delays maturation of the phagosome. J Cell Sci 110:731–743. https://doi.org/10.1242/jcs.110.6.731.
57. Alvarez-Dominguez C, Madrazo-Toca F, Fernandez-Prieto L, Vandekerckhove J, Pareja E, Tobes R, Gomez-Lopez MT, Del Cerro-Vadillo E, Fresno M, Leyva-Cobián F, Carrasco-Marín E. 2008. Characterization of a Listeria monocytogenes protein interfering with Rab5a. Traffic 9:325–337. https://doi.org/10.1111/j.1600-0854.2007.00683.x.
58. Christoforidis S, McBride HM, Burgoyne RD, Zerial M. 1999. The Rab5 effector EEA1 is a core component of endosome docking. Nature 397:621–625. https://doi.org/10.1038/17618.
59. Langemeyer L, Fröhlich F, Ungermann C. 2018. Rab GTPase function in endosome and lysosome biogenesis. Trends Cell Biol 28:957–970. https://doi.org/10.1016/j.tcb.2018.06.007.
60. Borchers AC, Langemeyer L, Ungermann C. 2021. Who's in control? Principles of Rab GTPase activation and endolysosomal membrane trafficking and beyond. J Cell Biol 220:e202105120. https://doi.org/10.1083/jcb.202105120.
61. Nordmann M, Cabrera M, Perz A, Bröcker C, Ostrowicz C, Engelbrecht-Vandré S, Ungermann C. 2010. The Mon1-Ccz1 complex is the GEF of the late endosomal Rab7 homolog Ypt7. Curr Biol 20:1654–1659. https://doi.org/10.1016/j.cub.2010.08.002.

62. Langemeyer L, Borchers AC, Herrmann E, Füllbrunn N, Han Y, Perz A, Auffarth K, Kümmel D, Ungermann C. 2020. A conserved and regulated mechanism drives endosomal Rab transition. eLife 9:e56090. https://doi.org/10.7554/eLife.56090.
63. Lawrence G, Brown CC, Flood BA, Karunakaran S, Cabrera M, Nordmann M, Ungermann C, Fratti RA. 2014. Dynamic association of the PI3P-interacting Mon1-Ccz1 GEF with vacuoles is controlled through its phosphorylation by the type 1 casein kinase Yck3. Mol Biol Cell 25:1608–1619. https://doi.org/10.1091/mbc.E13-08-0460.
64. Cabrera M, Nordmann M, Perz A, Schmedt D, Gerondopoulos A, Barr F, Piehler J, Engelbrecht-Vandré S, Ungermann C. 2014. The Mon1-Ccz1 GEF activates the Rab7 GTPase Ypt7 via a longin-fold-Rab interface and association with PI3P-positive membranes. J Cell Sci 127:1043–1051. https://doi.org/10.1242/jcs.140921.
65. Bohdanowicz M, Grinstein S. 2010. Vesicular traffic: a Rab SANDwich. Curr Biol 20:R311–R314. https://doi.org/10.1016/j.cub.2010.02.030.
66. Law F, Seo JH, Wang Z, DeLeon JL, Bolis Y, Brown A, Zong WX, Du G, Rocheleau CE. 2017. The VPS34 PI3K negatively regulates RAB-5 during endosome maturation. J Cell Sci 130:2007–2017. https://doi.org/10.1242/jcs.194746.
67. Weber SS, Ragaz C, Hilbi H. 2009. Pathogen trafficking pathways and host phosphoinositide metabolism. Mol Microbiol 71:1341–1352. https://doi.org/10.1111/j.1365-2958.2009.06608.x.
68. Alix E, Mukherjee S, Roy CR. 2011. Subversion of membrane transport pathways by vacuolar pathogens. J Cell Biol 195:943–952. https://doi.org/10.1083/jcb.201105019.
69. Fratti RA, Backer JM, Gruenberg J, Corvera S, Deretic V. 2001. Role of phosphatidylinositol 3-kinase and Rab5 effectors in phagosomal biogenesis and mycobacterial phagosome maturation arrest. J Cell Biol 154:631–644. https://doi.org/10.1083/jcb.200106049.
70. Fratti RA, Chua J, Vergne I, Deretic V. 2003. *Mycobacterium tuberculosis* glycosylated phosphatidylinositol causes phagosome maturation arrest. Proc Natl Acad Sci U S A 100:5437–5442. https://doi.org/10.1073/pnas.0737613100.
71. Vergne I, Fratti RA, Hill PJ, Chua J, Belisle J, Deretic V. 2004. *Mycobacterium tuberculosis* phagosome maturation arrest: mycobacterial phosphatidylinositol analog phosphatidylinositol mannoside stimulates early endosomal fusion. Mol Biol Cell 15:751–760. https://doi.org/10.1091/mbc.e03-05-0307.
72. Vergne I, Chua J, Lee HH, Lucas M, Belisle J, Deretic V. 2005. Mechanism of phagolysosome biogenesis block by viable *Mycobacterium tuberculosis*. Proc Natl Acad Sci U S A 102:4033–4038. https://doi.org/10.1073/pnas.0409716102.
73. Hernandez LD, Hueffer K, Wenk MR, Galan JE. 2004. *Salmonella* modulates vesicular traffic by altering phosphoinositide metabolism. Science 304:1805–1807. https://doi.org/10.1126/science.1098188.
74. Mallo GV, Espina M, Smith AC, Terebiznik MR, Aleman A, Finlay BB, Rameh LE, Grinstein S, Brumell JH. 2008. SopB promotes phosphatidylinositol 3-phosphate formation on *Salmonella* vacuoles by recruiting Rab5 and Vps34. J Cell Biol 182:741–752. https://doi.org/10.1083/jcb.200804131.
75. Ripio MT, Dominguez-Bernal G, Lara M, Suarez M, Vazquez-Boland JA. 1997. A Gly145Ser substitution in the transcriptional activator PrfA causes constitutive overexpression of virulence factors in *Listeria monocytogenes*. J Bacteriol 179:1533–1540. https://doi.org/10.1128/jb.179.5.1533-1540.1997.
76. Suarez M, Gonzalez-Zorn B, Vega Y, Chico-Calero I, Vazquez-Boland JA. 2001. A role for ActA in epithelial cell invasion by *Listeria monocytogenes*. Cell Microbiol 3:853–864. https://doi.org/10.1046/j.1462-5822.2001.00160.x.
77. Haima P, van Sinderen D, Schotting H, Bron S, Venema G. 1990. Development of a beta-galactosidase alpha-complementation system for molecular cloning in *Bacillus subtilis*. Gene 86:63–69. https://doi.org/10.1016/0378-1119(90)90114-7.
78. Arnaud M, Chastanet A, Debarbouille M. 2004. New vector for efficient allelic replacement in naturally nontransformable, low-GC-content, gram-positive bacteria. Appl Environ Microbiol 70:6887–6891. https://doi.org/10.1128/AEM.70.11.6887-6891.2004.
79. Pogulis RJ, Vallejo AN, Pease LR. 1996. *In vitro* recombination and mutagenesis by overlap extension PCR. Methods Mol Biol 57:167–176. https://doi.org/10.1385/0-89603-332-5:167.
80. Schröder A, Schröder B, Roppenser B, Linder S, Sinha B, Fässler R, Aepfelbacher M. 2006. *Staphylococcus aureus* fibronectin binding protein-A induces motile attachment sites and complex actin remodeling in living endothelial cells. Mol Biol Cell 17:5198–5210. https://doi.org/10.1091/mbc.e06-05-0463.
81. Fernandez-Mora E, Polidori M, Lührmann A, Schaible U, Haas A. 2005. Maturation of *Rhodococcus equi*-containing vacuole is arrested after completion of the early endosome stage. Traffic 6:635–653. https://doi.org/10.1111/j.1600-0854.2005.00304.x.
82. Lanahan SM, Wymann MP, Lucas CL. 2022. The role of PI3Kγ in the immune system: new insights and translational implications. Nat Rev Immunol 22:687–700. https://doi.org/10.1038/s41577-022-00701-8.